



RESEARCH ARTICLE

A NOVEL AND EFFICIENT PHOTOCATALYSIS (ZnO/BENTONITE) FOR
DISINFECTION OF *Escherichia coli* AND *Pseudomonas aeruginosa* UNDER VISIBLE LIGHT
IRRADIATION

Öge ARTAGAN ^{1,*} , Ali İmran VAİZOĞULLAR ¹ 

¹ Medical Service and Techniques Department, Vocational School of Health Services,
Muğla Sıtkı Koçman University, Muğla, Turkey

ABSTRACT

In the present study, a new composite catalyst which highly active under the visible light was synthesized by immobilizing onto bentonite surface using ZnO materials (ZnO/Bent). For this, a simple in situ participant technique was used. The samples were characterized using SEM, XRD, BET techniques. SEM images possess that ZnO particles have nearly a spherical structure. Bentonite clay was used to increase the surface area of the samples. The obtained BET surface area of the samples shows that the ZnO/Bent catalyst was lower than that of pure Bentonite. The aim of this study was to evaluate the effectiveness of photocatalytic disinfection with ZnO-Bent composite against *Escherichia coli* and *Pseudomonas aeruginosa* under visible light. The obtained results show that when *E. coli* strain was subjected to ZnO-Bent mediated photocatalytic disinfection under solar irradiation, more than 98 % disinfection of the targeted *E. coli* was achieved within 2 hours and also 100% of *P. aeruginosa* colonies were inactivated within 4 hours under solar irradiation. A Possible degradation mechanism for ZnO/Bent composite was proposed in this study.

Keywords: Antimicrobial Disinfection, Photocatalysis, ZnO-Bent, *Escherichia coli*, *Pseudomonas aeruginosa*

1. INTRODUCTION

Recently, toxic organic compounds that come from industrial development have caused a great environmental problem. Thus, the removal of these pollutants has become a major problem in scientific research. These organic toxic compounds negatively affect the human, environment and other organism's health in nature [1]. Every year, so many people are affected by contaminations of microorganisms (viral, bacterial) in the environment. Especially intestinal infections caused by contaminated water have also become leading causes of malnutrition and poor digestion [2]. The technology has the potential to provide an alternative method against the spread of infections, especially in view of the progress of visible light-activated catalysts. Photocatalysis has much more attention attracted worldwide due to its potential to inactivate a wide variety of microorganisms, by using solar energy. Photocatalysis is a safe, non-toxic, and rather cheap disinfection method and also adaptability allows it to be used for many purposes. Photocatalysis is a viable alternative technology for water treatment, indoor air, medical equipment disinfection, pharmaceuticals, food industry, plant protection, wastewater purification systems, drinking water disinfection largely because of its potential use. Direct solar energy success both disinfection and chemical detoxification [3, 4, 5, 6]. Disinfection of microorganisms by photocatalysis is of particular importance when compared to traditional chemical applications. Chlorination and other chemical applications have so many disadvantages. For instance, using chlorine for disinfection may regenerate organics in the water to chloro-organic compounds which are quite carcinogenic [7, 8]. Another thought of the traditional disinfection method is that pathogens and their cysts tend to develop resistance to chlorine disinfection or require higher doses for complete disinfection [7-10]. Different alternatives of disinfection for instance ozonation and irradiation have

some limitations, for instance, the lack of residual effect [11] and generation of colony alternatives [6, 12, 13]. Bentonite is a silicate-based clay mineral. It has a large specific surface area and great absorption property. Some researchers expressed that bentonite based ZnO is an efficient composite photocatalyst. It can have degraded organic toxins in the water medium. Also, Bentonite can effectively light absorption in the visible region. This caused more photoactive performance for ZnO/Bent photocatalysts sample [15]. There are so many studies about photocatalytic disinfection. For example, Sun and co-workers were studied the disinfections of *Aspergillus flavus*. They expressed that as synthesized composites were composed of rhombic NiFe₂O₄ nanosheets and g-C₃N₄ nanosized sheets, and 0.2 g-C₃N₄/NiFe₂O₄ (mass ratio) demonstrated the perfect activity with above 90% disinfection rate under 90 minutes visible light irradiation. The efficient disinfection performance was attributed to the supportive charges' separation, fine photoelectric properties and proper band structure [16]. Another work was performed by Najma and co-workers [17]. They stated that the structure and morphology of ZnO has an effective catalytic surface due to the hierarchical porosity and membrane formation on AAO substrates which showed a strong catalytic performance against E-coli. They also stated that the obtained results facilitated the transfer and diffusion of Zn²⁺ by the oxygen species in the reaction medium together with the large catalytic surface [17]. The study about the effective catalytic performance of zinc against some bacteria when in composite form was carried out by Karunakaran and co-workers. According to their findings, the incorporation of ZnO in TiO₂ has higher charge transfer resistance and lower capacitance under visible light [18]. The above studies have shown that photocatalytic disinfection processes can be applied by so many materials.

In the present study, ZnO and bentonite supported ZnO was synthesized by facile precipitation method. The visible light utility photocatalytic disinfection of microorganisms by ZnO/Bent composite. ZnO/Bent photocatalytic disinfection model has not been used against *E. coli* and *P. aeruginosa* until this time.

2. MATERIAL AND METHOD

All materials were of analytical grade except Bentonite, and they were used without purification. Firstly, 12.5 ml of ethylene glycol, 4,5 g of Zn (NO₃)₂·2H₂O were added to 50 ml of water and stirred for 30 min at 40°C (Solution A). simultaneously, 44 ml of LiOH solution (0.1 mol/L⁻¹) was added to solution A. Cloudy like Zn (OH)₂ was obtained onto Bentonite surface and stirred for 3 h. Hexane was added to ZnO sol to store for a night at 5°C. the white gel and then centrifuged and rinsed with distilled water. The obtained particle was dried at 80°C and calcined at 300°C for 3 hours. Bare ZnO nano spherics were synthesized as defined above procedure without the addition of bentonite.

The crystalline phase was examined by XRD (Rigaku Dmax 350) using copper K radiation ($\lambda=0.154056$ nm). The microstructure and shape of the particle were researched using SEM (JEOL JSM-7600F). The element was determined with (JEOL JSM-7600F) EDAX analyzer with SEM measurement. The Brunauer-Emmett-Teller (BET), pore-volume, and pore size were measured using ASAP2010 (Micromeritics Instrument Corporation, USA) with N₂ adsorption at 77.35 K.

2.1. Antimicrobial Activity on Bio ball

The antimicrobial susceptibility profile of ZnO-Bent was determined by the Spreading Plate method. BioBall MultiShot 10E8 is a freeze-dried water-soluble ball containing a precise number of viable cells. BioBall is produced to the world's highest quality standards, achieving ISO Guide 34, a standard for reference material producers, accreditation. Each BioBall was rehydrated in 1.1 mL Re-Hydration Fluid containing 10 doses of 100 uL with 10⁷ cfu each, resulting in a target concentration of 5 × 10⁵ cfu per mL when inoculated in 20 mL of Nutrient Broth (NB) [13]. Activated bacteria were used in the Spreading Plate method [14].

2.2. Bacterial Strains and Growth Conditions

E. coli (NCTC 12923), *P. aeruginosa* (NCTC 12924) BioBall MultiShot 10E8 were used. Nutrient agar for bacteria was prepared and diluted to 25 ml of petri dishes for the purpose of studying the surviving microorganisms. The material was weighed at 250 µg/mL and incubated with microorganisms. At the 2nd, 4th and 6th hours samples were taken, incubated in daylight, specimens taken, transferred to new petri dishes and incubated for 24 hours at 37 ° C, then the colonies were counted with the help of a magnifying glass.

3. RESULTS

3.1.XRD Analysis

Figure 1 shows the XRD patterns of Bent, ZnO and ZnO-Bent materials. From Figure 1, the characteristic peak of bentonite at 21.81°, 27.62 and 35.88 2θ degrees are seen in the Bentonite structure. The peaks appear at 2θ=31.83, 34.45, 36.28, 47.56 are shown in ZnO-Bent pattern which is wurtzite structure of ZnO indexed as (1 0 0), (0 0 2), (1 0 1), (1 0 2) plane respectively [19]. Also, bentonite and no peaks are obtained in the ZnO-Bent XRD sample [20].

The intensity of major peaks of ZnO decreased in ZnO/Bent sample. The decrease in diffraction peaks of ZnO was related to the interaction between Bentonite and ZnO oxides. These results confirmed that ZnO dispersed onto the Bentonite surface effectively. The calculated particle size of ZnO and ZnO-Bent from the Debye-Scherer equation was obtained to be 30, 50 and 80 nm approximately.

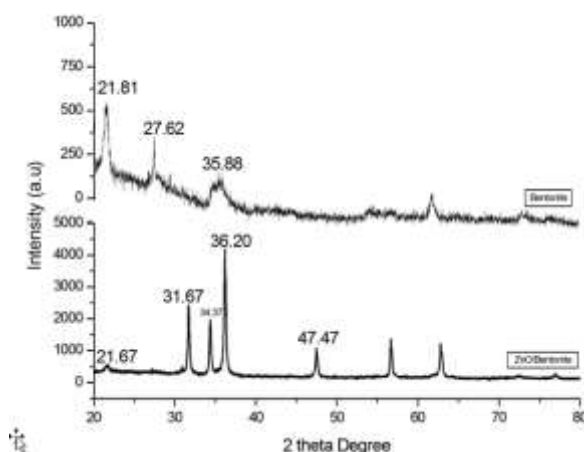
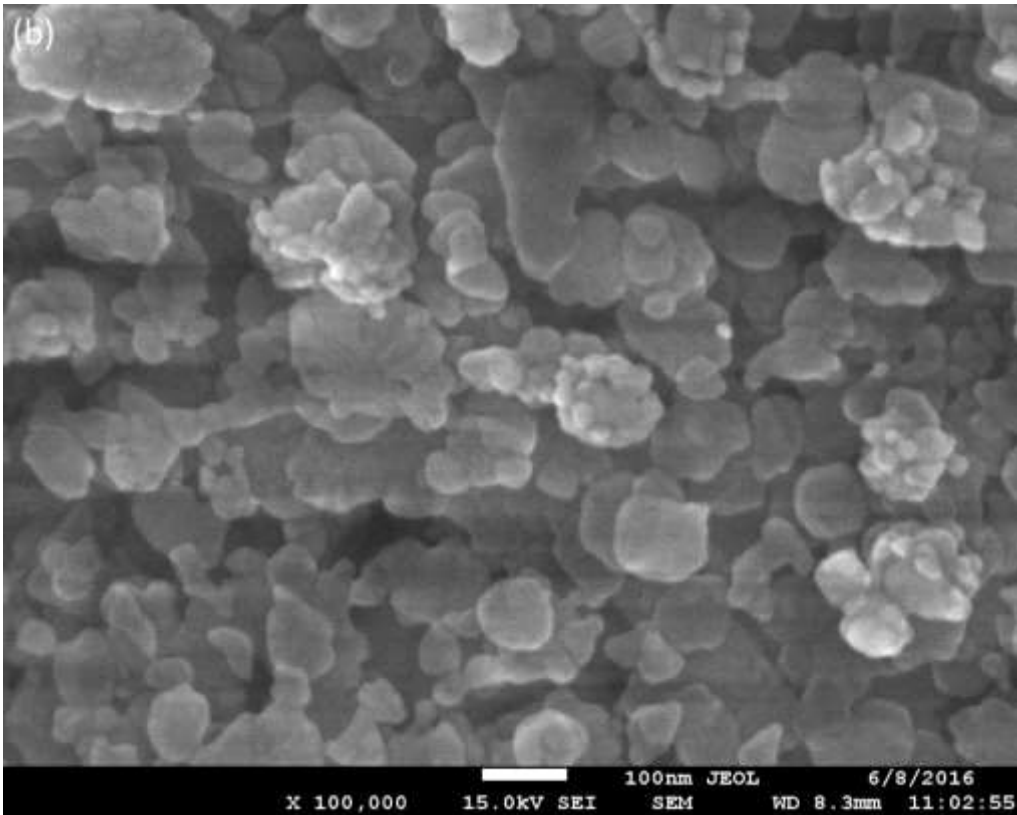
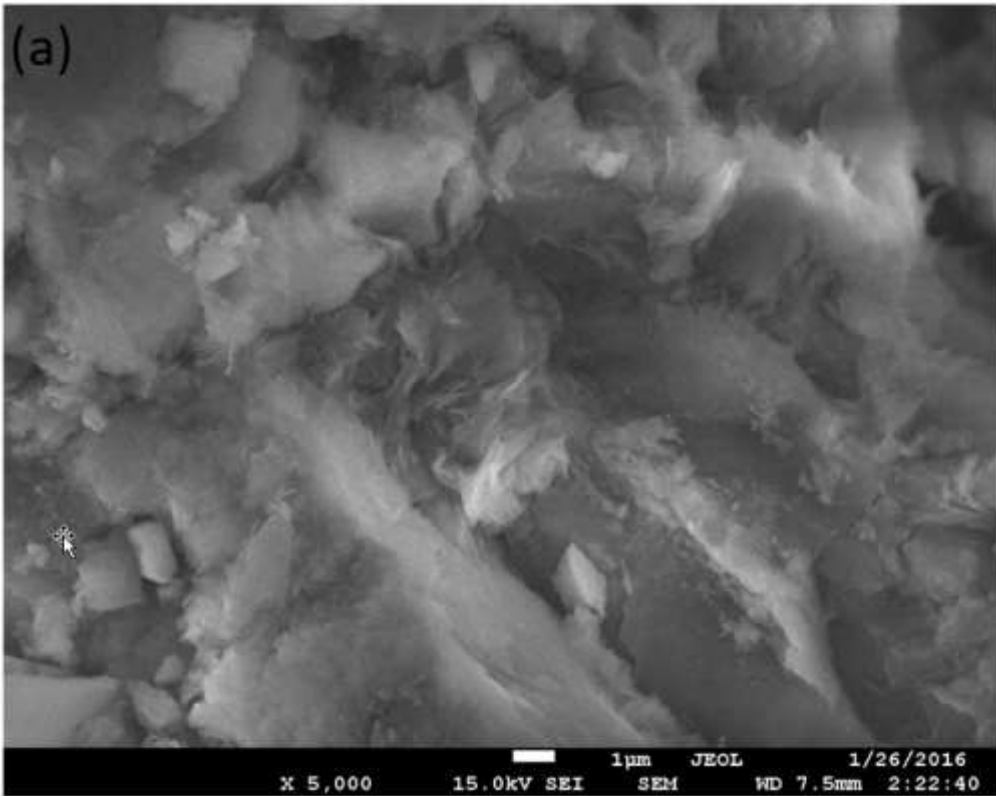


Figure1. XRD pattern of Bentonite and ZnO/Bent catalysts

3.2. SEM and BET Analysis

SEM analyses of the samples are presented in Figure 2. From Figure2, bentonite clay has cottony-like structure. ZnO particles displayed nano spherical morphology. In addition, the SEM image of the ZnO-Bentonite catalyst exhibited the same morphology with the ZnO. This indicated that bentonite clay did not change the ZnO morphology. However, the particle size of the ZnO decreased after immobilization onto the bentonite surface. This confirmed that effective dispersion caused lower particle aggregation energy. The BET surface areas of the synthesized catalysts are shown in Table 1. From table 1, as seen, the BET surface area of the ZnO-Bent sample decreased effectively confirming the excellent dispersion onto the bentonite surface.



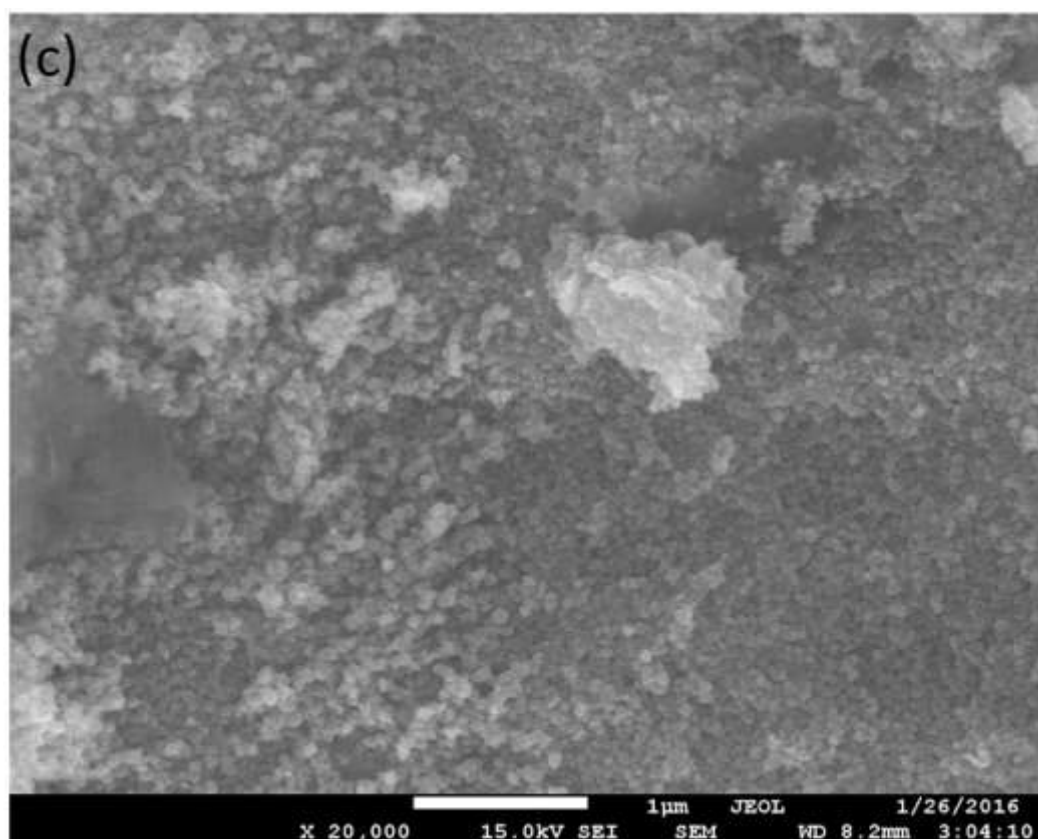


Figure 2. SEM images of Bentonite (a), ZnO (b) and ZnO/Bent (c) catalysts

Table 1. Textural and pseudo first-order data of the synthesized catalysts

Sample	BET (m ² /g)	Pore volume (cm ³ /g)	Pore size (nm)
Bentonite	125.25	1.689	17.98
ZnO	2.563	0.055	1.295
ZnO-Bent	56.10	0.158	11.622

3.3. UV-DRS analysis and Structural Properties

Figure 3 presents the UV-DRS spectra of the ZnO and ZnO-Bent samples. As seen that both samples show a strong absorbance between 300-400 nm. The absorption spectrum of ZnO shifted to a higher wavelength when it was loaded onto bentonite clay. The edge of the bandgap of ZnO and ZnO/Bent are 381 and 406 nm respectively. The bandgap energy which can be calculated from the onset of the absorption edge (λ_g) using the $E_g = 1240/\lambda_g$ the formula is 3.25 and 3.05 eV for the ZnO and ZnO/Bent catalysts respectively (redshift). These results are likely to be related to crystallite defects after dispersed onto the bentonite surface. This also shows that bentonite assisted ZnO (ZnO-Bent) has useful for the degradation of hazardous under visible light [21].

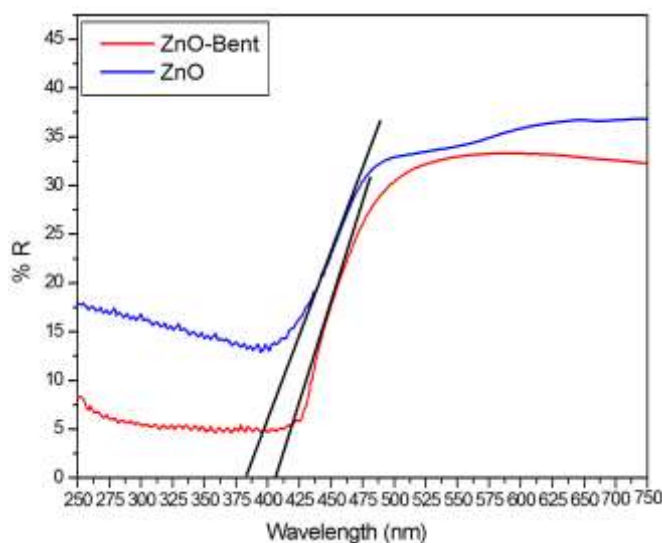


Figure 3. UV-DRS spectra of the samples

Photocatalytic mechanism has been potential of inactivation of diverse microorganisms such as bacteria (gram-positive and negative), endospores, fungi, algae, protozoa, viruses. Photocatalysis has also been shown to be capable of inactivating prions [24]. Foster and friends (2011) reported that; In recent years, there has been a significant increase in the number of publications referring to photocatalytic disinfection models [25].

Mahon and friends investigated the performance of photocatalytic treatment processes by using different photocatalysts against *E. coli* and bacteriophages MS2, Φ X174 and PR772, under real sunlight conditions [26].

Oh, and friends investigated the antibacterial activity of the CuBi₂O₄ composites (i.e. CuO–CuB, CuO–CuB–EG, CuO₂–CuB–EG and CuO₃–CuB–EG) against *E. coli*. *E. coli* (major group of Gram-negative bacteria) was selected as the model pathogenic organism [27].

The performance of the photocatalytic treatment process was assessed using ZnO-Bent photocatalysts against *E. coli* and *P. aeruginosa*. Figure 5 shows a plate with *E. coli* colonies in the initial concentration sample, as a control. Photocatalytic disinfection by ZnO- Bent against *E. coli* reached the max level within 2 hours (Figure 5-6). Within 2 hours of photocatalysis, 98.3 % (Table 3) of *E. coli* inactivation was achieved and then within 4 hours of photocatalysis with daylight, 89% (detailed in table 3) of *E. coli* was inactivated (Figure 6). Figure 6 shows that there has been a sharp drop in the number of *E. coli* colonies within 2 hours of ZnO-Bent photocatalyst activity.

Figure 7 shows a plate with *P. aeruginosa* colonies in the initial concentration sample, as a control. After 2 hours of irradiation with visible light 86% of *P. aeruginosa* were inactivated. Photocatalytic disinfection by ZnO- Bent against *P. aeruginosa* reached the maximum level within 4 hours (Figure 7-8).

The antibacterial potential of ZnO-Bent under visible light irradiation was detailed in Table 3. ZnO-Bent photocatalytic activity was evaluated by the inactivation of *E. coli* and *P. aeruginosa*. The experimental results showed that ZnO-Bent inactivated 98.3% of *E. coli* colonies within 2 hours incubation and inactivated 100 % of *P. aeruginosa* colonies within 4 hours (Table 3).

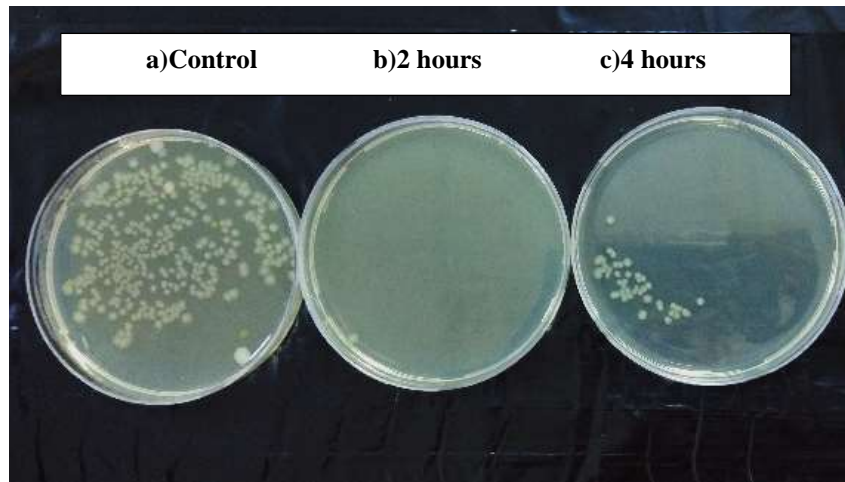


Figure 5. Antimicrobial effects of ZnO-Bent against *E. coli* colonies. *E. coli* cultivated plates incubated ZnO-Bent: a) Control, b) 2 hours of incubation with Zno-Bent, c) 4 hours of incubation with Zno-Bent photocatalyst.

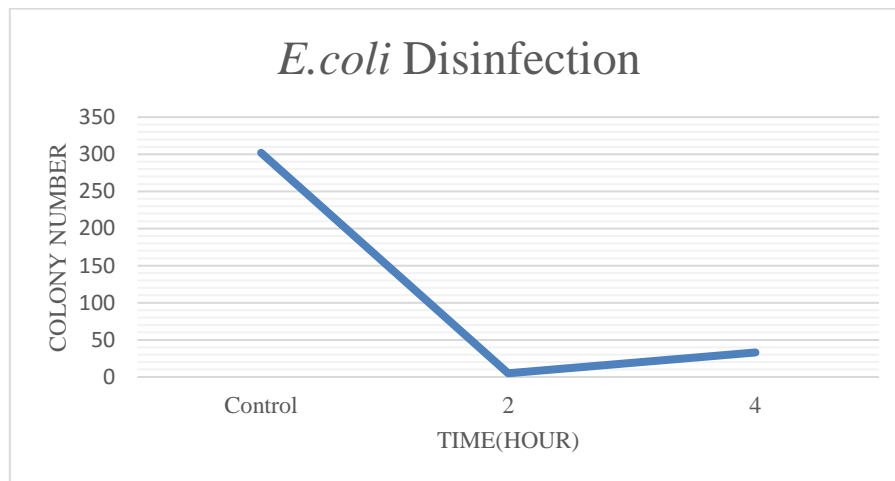


Figure 6. The antimicrobial capacity of ZnO-Bent photocatalys activity under visible light.

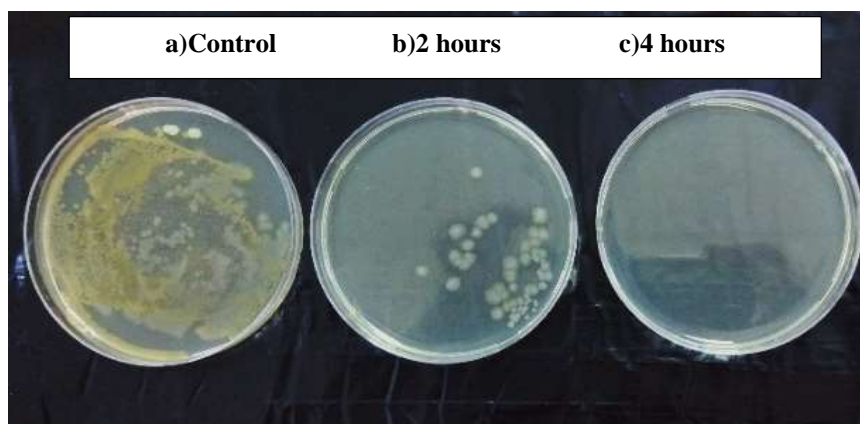


Figure 7. Antimicrobial effects of ZnO-Bent against *P. aeruginosa* Colonies. *P. aeruginosa* cultivated plates incubated ZnO-Bent: a) Control, b) 2 hours of incubation with Zno-Bent, c) 4 hours of incubation with Zno-Bent photocatalyst.

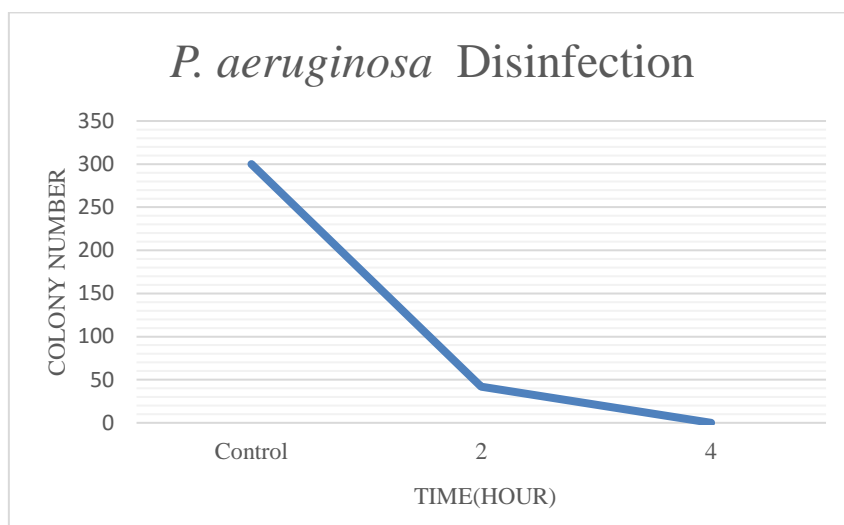


Figure 8. The antimicrobial capacity of ZnO-Bent photocatalyst activity under visible light is presented in a time-dependent manner.

Table 3. Microbicide activities of ZnO-Bent against *E. coli* and *P. aeruginosa* respectively.

	<i>E. coli</i> (2 hours incubation)	<i>E. coli</i> (4 hours incubation)	<i>P. aeruginosa</i> (2 hours incubation)	<i>P. aeruginosa</i> (4 hours incubation)
ZnO-Bent	%98.3	%89	%86	%100

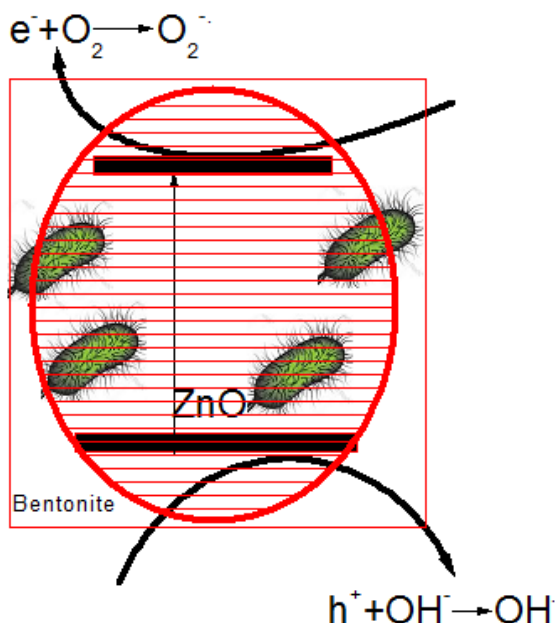


Figure 9. Photocatalytic illustration of disinfection of e-coli under visible light

From Figure 9 when excited the ZnO-Bent catalyst under visible light the valence band electrons transferred to its conductive band level. In this case, the charge carriers which are holes and electrons reacted with H_2O and O_2 to form hydroxide (OH^-) and superoxide ($O_2^{\cdot-}$) radicals respectively [22]. This oxidation process caused to inactivate the *E. coli* and *P. aeruginosa* [23].

4. DISCUSSION

ZnO/Bent photocatalytic inactivation performance against *P. aeruginosa* was highest at the end of 4 hours. ZnO/Bent photocatalytic inactivation performance against *E. coli* was highest at the end of 2 hours. In summary, as synthesized ZnO/Bent particles were spherical morphology with cotton-like bentonite. the ZnO/Bent catalyst was fabricated by introducing the ZnO compound onto the Bentonite surface. The photocatalytic performance of as-synthesized catalysts shows that ZnO/Bent composite exhibits better photoactivity than pure ZnO under visible light. Based on the above results, the enhanced photocatalytic activity for the ZnO/Bent catalyst can be attributed to two major factors. The first one is the efficient inhibition of recombination rate of e^-/h^+ pairs. This caused more radicals available on the catalyst surface to inactivate the *E. coli* and *P. aeruginosa*. The second one is the higher adsorption ability in the ZnO/Bent system. Photocatalytic mechanism efficiency depends on the particle size of the composite and microorganism type. This research exhibits the efficiency of ZnO/Bent photocatalytic disinfection model against *E. coli* and *P. aeruginosa*. Manuscript expected to offer useful perspectives for the future improvements in this research area.

ACKNOWLEDGMENTS

This study has been supported by Mugla Sıtkı Koçman University Scientific Research Unit with 15/139

CONFLICT OF INTEREST

The authors stated that there are no conflicts of interest regarding the publication of this article.

REFERENCE

- [1] Zhang G, Tan Y, Sun Z, Zheng S. Synthesis of BiOCl/TiO₂ heterostructure composites and their enhanced photocatalytic activity. J Environ Chem Eng, 2017; 5: 1196-1204.
- [2] Lima AAM, Moore SR, Barboza MS, et al. Persistent Diarrhea Signals a Critical Period of Increased Diarrhea Burdens and Nutritional Shortfalls: A Prospective Cohort Study among Children in Northeastern Brazil. The Journal of Infectious Diseases, 2000; 181(5): 1643-1651.
- [3] Singh P, Bengtsson L. Impact of warmer climate on melt and evaporation for the rainfed, snowfed and glacierfed basins in the Himalayan region. Journal of Hydrology, 2005; 300:140-154.
- [4] Shannon M, Bohn PW, Elimelech M, Georgiadis JG, Mariñas BJ, Mayes AM, Science and technology for water purification in the coming decades. Nature, 2008; 452: 301-310.
- [5] Wang W, Huang G, Jimmy CY, Wong PK. Advances in photocatalytic disinfection of bacteria: development of photocatalysts and mechanisms. Journal of Environmental Sciences, 2015; 34: 232-247.
- [6] Gamage J, Zhang Z. Applications of photocatalytic disinfection. International Journal of Photoenergy, 2010; 1-10.
- [7] Song L, Pang Y, Zheng Y, et al. Design, preparation and enhanced photocatalytic activity of porous BiOCl/BiVO₄ microspheres via a coprecipitation-hydrothermal method. Journal of Alloys and Compounds, 2017; 710, 375-382.
- [8] Zhang L, Wang W, Zhou L, Shang M & Sun S, Fe₃O₄ coupled BiOCl: a highly efficient magnetic photocatalyst. Appl Catal B, 2009; 90 (3-4): 458- 462.

- [9] Zhang KL, Liu CM, Huang FQ et al. Study of the electronic structure and photocatalytic activity of the BiOCl photocatalyst. *Appl. Catal. B Environ*, 2006; 68 (3-4): 125–129.
- [10] Liu Y, Yao W, Liu D, et al. Enhancement of visible light mineralization ability and photocatalytic of $\text{BiPO}_4/\text{BiOI}$. *Appl. Catal. B: Environ* 2015; 163: 547-553.
- [11] Ma W, Chen L, Zhu Y, et al. Facile synthesis of the magnetic $\text{BiOCl}/\text{ZnFe}_2\text{O}_4$ heterostructures with enhanced photocatalytic activity under visible light irradiation. *Colloids And Surfaces A: Physicochem And Eng. Aspects*, 2016; 508: 135-141.
- [12] Priya B, Shandilya P, Raizada P, et al. Photocatalytic mineralization and degradation kinetics of ampicillin and oxytetracycline antibiotics using graphene sand composite and chitosan supported BiOCl. *J. Mol.Catal. A: Chemical*, 2016; 423: 400-413.
- [13] Zhang L, Zhang J, Zhang W, et al. Photocatalytic activity of attapulgite-BiOCl-TiO₂ toward degradation of methyl orange under UV and visible light irradiation. *Mater Res Bull*, 2015; 66: 109-114.
- [14] Hartman D, Perfecting Your Spread Plate Technique. *J Microbiol Biol Educ*. 2011; 12(2): 204-205.
- [15] Saelim NO, Magaraphan R, Sreethawong T. Preparation of sol-gel TiO₂/purified Na-bentonite composites and their photovoltaic application for natural dye-sensitized solar cells. *Energy Convers Manage*, 2011; 52(8–9): 2815–2818.
- [16] Sun D, Mao J, Cheng L, Yang X, Li H, Zhang L, Zang W, Zang Q, Li P, Magnetic g-C₃N₄/NiFe₂O₄ composite with enhanced activity on photocatalytic disinfection of *Aspergillus flavus*. *Chemical Engineering Journal*, 2021; 418: 129417.
- [17] Najma B, Kasi AK, Kasi JK, Akbar A, Bokhari SMA, Stroe IR, ZnO/AAO photocatalytic membranes for efficient water disinfection: Synthesis, characterization and antibacterial assay. *Applied Surface Science*, 2018; 448:104-114.
- [18] Karunakaran C, Abiramasundari G, Gomathisankar P, Manikandan G, Anandi V, Preparation and characterization of ZnO–TiO₂ nanocomposite for photocatalytic disinfection of bacteria and detoxification of cyanide under visible light. *Materials Research Bulletin*, 2011; 46(10): 1586-1592.
- [19] Cao M, Wang F, Zhu J, et al. Shape-controlled synthesis of flower-like ZnO microstructures and their enhanced photocatalytic properties. *Materials Letters*, 2017; 192, 1-4.
- [20] Soltani, RDC, Jorfi S, Safari M, Rajaei MS, Enhanced sonocatalysis of textile wastewater using bentonite supported ZnO nanoparticles: Response surface methodological approach. *Journal of Environmental Management*, 2016; 179: 47-57.
- [21] Baikousi M, Bourlinos AB, Douvalis A, et al. Synthesis and characterization of $\gamma\text{-Fe}_2\text{O}_3$ /carbon hybrids and their application in the removal of hexavalent chromium ions from aqueous solutions. *Langmuir*, 2012; 28(8): 3918-3930.

- [22] Vaizoğullar Aİ, TiO₂/ZnO Supported on Sepiolite: Preparation, Structural Characterization, and Photocatalytic Degradation of Flumequine Antibiotic in Aqueous Solution. *Chem Eng Commun*, 2017; 204: 689-697.
- [23] Motshekga SC, Ray SS, Onyango MS, Momba MN, Microwave-assisted synthesis, characterization and antibacterial activity of Ag/ZnO nanoparticles supported bentonite clay. *Journal of Hazardous Materials*, 2013; 262: 439-446.
- [24] Paspaltsis I, Kotta K, Lagoudaki R, et al. Titanium dioxide photocatalytic inactivation of prions. *Journal of General Virology*, 2006; 87(10):3125–3130.
- [25] Foster HA, Ditta IB, Varghese S. Photocatalytic disinfection using titanium dioxide: spectrum and mechanism of antimicrobial activity. *Applied Microbiology Biotechnology*, 2011; 90:1847–1868
- [26] Mahon MJ, Pillai SC, Kelly JM, Gill LW. Solar photocatalytic disinfection of E. coli and bacteriophages MS2, ΦX174 and PR772 using TiO₂, ZnO and ruthenium-based complexes in a continuous flow system. *Journal of Photochemistry & Photobiology, B: Biology*, 2017; 170:79-90.
- [27] Oh W-D, Lua S-K, Donga Z, Lim T-T. Rational design of hierarchically structured CuBi₂O₄ composites by deliberate manipulation of the nucleation and growth kinetics of CuBi₂O₄ for environmental applications. *Nanoscale* 2016; 8:2046-2054.